Sensors and Actuators B 243 (2017) 946–954

Contents lists available at ScienceDirect

Sensors and Actuators B: Chemical

journal homepage: www.elsevier.com/locate/snb

A visual application of gold nanoparticles: Simple, reliable and sensitive detection of kanamycin based on hydrogen-bonding recognition

Lei Qin[a,b], Guangming Zeng[a,b,*], Cui Lai[a,b,*], Danlian Huang[a,b], Chen Zhang[a,b], Piao Xu[a,b], Tianjue Hu[a,b], Xigui Liu[a,b], Min Cheng[a,b], Yang Liu[a,b], Liang Hu[a,b], Yaoyu Zhou[c]

[a] College of Environmental Science and Engineering, Hunan University, Changsha, 410082, PR China
[b] Key Laboratory of Environmental Biology and Pollution Control, Hunan University, Ministry of Education, Changsha 410082, PR China
[c] College of Resources and Environment, Hunan Agricultural University, Changsha, Hunan, 410128, PR China

ARTICLE INFO

Article history:
Received 9 September 2016
Received in revised form
14 December 2016
Accepted 15 December 2016
Available online 18 December 2016

Keywords:
Kanamycin
Hydrogen-bonding recognition
Gold nanoparticles
4-Amino-3-hydrazino-5-mercapto-1, 2, 4-triazole
Sensor
Colorimetric

ABSTRACT

The authors here described a visual detection strategy employing 4-amino-3-hydrazino-5-mercapto-1, 2, 4-triazole (AHMT) functionalized gold nanoparticles (AuNPs) to detect kanamycin (KA) in various samples. The AHMT with mercapto group was self-assembled onto the surface of AuNPs and the AHMT functionalized AuNPs (AHMT-AuNPs) aggregated when KA existed owing to the hydrogen-bonding interaction between KA and AHMT. As a result, the color of the AHMT-AuNPs solution changed from wine red-to-deep purple with the increasing concentration of KA. Taking advantage of the hydrogen-bonding interaction, KA could be quantitatively detected by the proposed sensor in the range of 0.005–0.1 μM and 0.1–20 μM, with the detection limit as low as 0.004 μM which is much lower than the maximum contamination level for KA in milk defined by the European Union. Furthermore, the proposed sensor was not affected by the interference chemicals including common amine acid, antibiotics, and metal ions. The sensor was also used to detect KA from various real samples, and the results were excellent in accord with the values measured by the high performance liquid chromatography (HPLC). This sensor exhibited a promising potential for simple and real-time detection of KA in various real samples.

1. Introduction

Nano-sized precious metal particles, such as gold nanoparticles (AuNPs) and silver nanoparticles, have been manufactured and applied in many fields because of their unique optical characteristics [1,2]. As a visual element providing broad applications in chemistry, biology, medical, and material science, AuNPs have attracted much interest since the gold hydrosols were prepared by Michael Faraday in 1857 [3,4]. AuNPs supplied a spectral innovative approach for the sensing system owing to its unique optoelectronic properties, such as conductivity or redox behavior, surface plasmon resonance absorption, and resonance light scattering [5]. What is more remarkable is that the search for colorimetric detections based on AuNPs has been applied in many fields for their convenience of simple operations and visual observation [6,7]. For example, Elghanian et al. [8] reported a highly selective colorimetric polynucleotide detection approach based on a single-stranded target oligonucleotide (mercaptoalkyoligonucleotide) functionalized AuNPs probes. It provided the results with a concomitant red-to-pinkish/purple color change. In 2011, Guo et al. [9] developed a simple and simultaneous determination method of Hg^{2+}, Pb^{2+}, and Cu^{2+} using the papain-modified AuNPs with the lowest detection concentration of 200 nM. On this basis, our group has developed a papain and 2,6-pyridinedicarboxylic acid functionalized AuNPs (P-PDCA-AuNPs) sensor system for sensitive and selective detection of mercury ions based on the non-covalent reaction, with the linear range of 0.01–14 μM and detection limit of 9 nM [10]. Based on these promising results, AuNPs have been acknowledged as suitable for the detection of organic molecules.

In particular, many novel nanoparticle sensors for the identification of organic molecules have been developed by taking advantage of the color change of AuNPs induced by hydrogen-bonding recognition [11,12]. The hydrogen-bonding interaction is an attractive

* Corresponding authors at: College of Environmental Science and Engineering, Hunan University, Changsha, Hunan 410082, PR China.
E-mail addresses: zgming@hnu.edu.cn (G. Zeng), laicui@hnu.edu.cn (C. Lai).

http://dx.doi.org/10.1016/j.snb.2016.12.086
0925-4005/

interaction between a hydrogen atom from a molecule or a molecular fragment X-H and an atom or a group of atoms in the same or different. A typical hydrogen-bonding interaction may be depicted as X-H...Y, where X-H represents the donor and Y is the acceptor in which the change transfer presents between them leading to partial covalent bond formation between Y and H [13]. As for the applications of AuNPs based on hydrogen-bonding interaction, Ai et al. [14] developed a visual detection method of melamine in raw milk and infant formula based on hydrogen-bonding recognition-induced color change of AuNPs, which used the hydrogen-bonding interaction between melamine and the derivatives of cyanuric acid that could form a stable NH···O and NH···N hydrogen bonds. Then, a colorimetric sensor for clenbuterol using AuNPs in the presence of melamine was reported by Zhang and his group [11]. This paper described the hydrogen-bonding interaction between melamine and clenbuterol which led to the aggregation of AuNPs and a consequent color change. It is a new tendency of using AuNPs based on hydrogen-bonding interaction to identify organic molecules, especially antibiotics.

As a new kind of pollutants, antibiotics have attracted particular attention due to their broad applications and potential side effects [15]. Kanamycin (KA), an aminoglycoside antibiotic, is arising from the fermentation of *Streptomyces kanamyceticus* and used as a second-line antituberculosis drug because of its clinically useful activity against the *Mycobacterium tuberculosis* [16,17]. Similar to most of aminoglycoside antibiotics, indeed dependent side effects of nephrotoxicity, ototoxicity, and allergic reactions have been reported [18]. Besides, the residual amount of kanamycin in foodstuff may result in antibiotic resistance from the pathogenic bacterial strains, which could imperil the consumer [19]. Herein, an analytical method for the detection of kanamycin in various samples is still needed. Several methods, such as high performance liquid chromatographic methods [20,21], immunoassay [22], electrochemical detection [23], colorimetric detection [24,25], and gas chromatography [26] have been reported for the determination of kanamycin. Compared with these methods, colorimetric detection of kanamycin based on hydrogen-bonding interaction of functionalized AuNPs real-time analytical devices has many advantages, including simple, fast, low cost, high sensitivity, and selectivity. For example, Feng et al. [27] developed a practical colorimetric approach for the quantitation determination of dopamine in 2013, which was based on the hydrogen-bonding interaction between 4-amino-3-hydrazino-5-mercapto-1, 2, 4-triazol (AHMT) and dopamine. AHMT contains amino, hydrazine, mercapto, and trialzol groups, as the full name it is [28]. It can bind with AuNPs on the surface because of the mercapto-group [29]. On the other hand, the melamine molecule provides some hydrogen bond sites since it has three exocyclic amino groups and a three nitrogen hybrid ring, which is similar with AHMT [30]. Thus, AHMT can provide hydrogen bond sites.

In this study, a colorimetric sensor for kanamycin recognition based on AHMT functionalized AuNPs by the hydrogen-bonding interaction was developed. The determination of kanamycin in various samples was obtained and the sensitivity was satisfied. Many kinds of other organics were used here to illustrate the selectivity of this sensor system. In addition, high performance liquid chromatography (HPLC) was employed for the low levels of kanamycin to exhibit the accuracy of this method.

2. Materials and methods

2.1. Materials and instruments

Sodium citrate and chloroauric acid hydrated ($HAuCl_4{\cdot}4H_2O$) were obtained from Sinopharm Chemical Reagent Co., Ltd (Beijing, China). Kanamycin monosulfate ($KA{\cdot}H_2SO_4$) and 4-amino-3-hydrazino-5-mercapto-1, 2, 4-triazole (AHMT) were purchased from Xiya Chemical Industry Co., Ltd (Shandong, China). All of the other amino acids and carbohydrate used in this work, including L-aspartic acid, L-arginine, Glycine, L-phenylalanine, L-cysteine, Glutathione, Tetracycline, and Glucose, were received from Sigma-Aldrich (USA). Other chemicals involving metal ions salts were obtained from Damao Reagent of Tianjin (Tianjin, China). All the chemicals were of analytical grade and used without further purification. Ultrapure water (18.2 MΩ cm, Milli-Q Millipore) was used throughout the whole experiments. The buffer used in this work was 20 mM phosphate buffer (PB) (pH 7.4).

The size and the aggregation status of AHMT-stabilized gold nanoparticles were examined by the transmission electron microscopy (TEM) using TECNAI T20 G^2 electron microscope instrument operated at accelerating voltage of 200 Kv (FEI, Netherland). The UV–vis spectra of the sensor system were recorded by a UV-2005 spectrometer with a 1-cm path length quartz cuvette (Shimadzu Corporation, Kyoto, Japan). Pictures for color changes were taken with a Canon 70d digital camera. Zeta potential measurements were performed on a Zetasizer Nano ZS (England). High performance liquid chromatography (HPLC) was performed using an Agilent Technologies 1200 high performance liquid chromatography equipped with a UV–vis detector (DAD) and C18 column (4.6 mm × 250 mm, 5 μm). The mobile phase was acetonitrile/water (40/60, v/v) at the flow rate of 1 mL min^{-1}. The wavelength of UV detector was set at 230 nm and the injection volume was 50 μL.

2.2. Preparation of AHMT functionalized AuNPs

The glasswares were cleaned in a bath of freshly prepared 3:1 (V/V) HNO_3-HCl, amply rinsed with ultrapure water, and dried in the air. AuNPs used in this study were prepared by sodium citrate-mediated reduction of $HAuCl_4$ according to the literature [10,31] with a little modification. Briefly, 100 mL of 0.3 mM $HAuCl_4$ aqueous solution in a 250 mL round-bottom flask equipped with a condenser was heated to thorough boiling. Later, 15 mL of 38.8 mM sodium citrate was quickly added to the boiling solution with vigorous stirring. The color of the solution changed from light yellow to wine red within 3 min, which indicated the formation of AuNPs. The solution was cooled to room temperature under continuous stirring for 20 min and filtered through a 0.22-μm Millipore syringe filter. The resulting AuNPs were stored at 4 °C in the dark for further use. The average diameter of such AuNPs was ~15 nm through the measurement of TEM images and Zetasizer Nano ZS. The concentration of such prepared AuNPs was detected by UV–vis spectra according to Beer's law, using the molar extinction coefficients at the maximum absorption band of gold colloid [32]. The concentration of the prepared AuNPs was 10 nM.

The AuNPs functionalized with AHMT (AHMT-AuNPs) were obtained by adding (0.05 mM, 10 mL) AHMT to the AuNPs solutions (10 nM, 300 mL). The mixture was incubated in dark for 2 h under oscillation to ensure the functionalization of AHMT onto the surface of AuNPs. Then the AHMT-AuNPs solution was centrifuged at 12000 rpm for 20 min, and the deposition was washed for several times by ultrapure water to removal the excess AHMT in solution. After centrifuging, the sediment was resuspended to original volume with 20 mM PB. Consisting with the reported literature [27], the surface coverage ratio of AHMT-AuNPs is about 91.5%, which may attribute to both the nitrogen atom and −SH of AHMT can combine with AuNPs on the surface. Hence, the prepared AHMT-AuNPs were with good stability and then characterized by TEM and UV–vis microscopy. The pH of the solution controlled using the PB (20 mM, pH 7.4).

2.3. Colorimetric detection of KA in various samples

Colorimetric detection of KA was used to evaluate the range of detection concentration of KA with the AHMT-AuNPs system. Typically, different concentrations of analytes were added to 2 mL of prepared AHMT-AuNPs solution in a 5 mL sample bottle and then incubated at room temperature for 10 min. The color change of the mixtures was observed with the naked eye and recorded with a digital camera. The absorbance spectra were performed with a UV–vis spectrometer over the wavelength range from 200 to 800 nm. The aggregation kinetics at different concentrations of KA analyte was obtained through the absorption ratio of A_{650}/A_{520}. In order to testify the hydrogen-bonding interaction between AHMT and KA, the potential of different concentrations of KA with AHMT-AuNPs system was detected using a Zetasizer Nano ZS. To evaluate the selectivity, several similar materials were tested using the AHMT-AuNPs system, including organic molecules (Tetracycline, L-arginine, L-aspartic acid, Glucose, Glutathione, Glycine, L-lysine, and L-phenylalanine) and metal ions (Na^+, K^+, Mg^{2+}, and Ca^{2+}). The concentration of these molecules in the control experiments was 20 μM, and then the UV–vis spectra were recorded in 10 min.

2.4. Extract of various real samples

In the first place, different kinds of water samples including tap water, drinking water, river water, and pond water were collected from our laboratory, office, the Hsiang River (Changsha, China), and Lake of Peach (Changsha, China), respectively. All of these water samples were filtered through a 0.22 μm syringe filter and centrifuged for 20 min at 12000 rpm before the detection measurements were performed. Then, the contents of KA in these samples were measured by HPLC. Finally, the samples were prepared via spiking with the standard solutions of KA and stored at 4 °C for further analysis. Secondly, the milk without KA was bought from a local supermarket and the urine was collected from a pig (in a local pig farm) and directly measured by HPLC. Then, the samples were diluted for 100-fold and spiked with the standard solutions of KA for validating the effectiveness of the colorimetric detection of KA in real samples. After that, the samples were filtered and stored in accord with the aforementioned process.

3. Results and discussion

3.1. Mechanism of proposed sensor for KA detection

The surface attachment of mercapto group and electron-rich nitrogen-containing ligands on AuNPs has been well developed [9,33]. On one hand, AHMT contains one mercapto group, which can strongly coordinate to the surface of AuNPs. In addition, AHMT has two exocyclic amino groups and a three nitrogen hybrid ring, which is similar with melamine. Literatures reported that melamine has been widely used as a gelling component since it contains nine hydrogen bonding sites in its molecule [30,34]. AHMT has the same property as melamine according to the studies of Feng et al. [35] and Chen et al. [36]. On the other hand, as an aminoglycoside antibiotic, KA has four amino groups (-NH_2) and seven hydroxyl groups (-OH) which may combine with the AHMT through hydrogen-bonding interaction. As described in Scheme 1, the as-prepared AHMT-AuNPs solution is stable and well dispersed, owing to the electrostatic repulsion of the positive capping agent against the van der Waals attraction. When the KA exists, the hydrogen-bonding interaction comes about and induces the collective oscillations of the surface electron, which results in the aggregation of AHMT-AuNPs and a series of color change.

In order to verify the speculation, the design was applied to recognize KA via AHMT functionalized AuNPs. After addition of AHMT, little difference of the color change was observed with the naked eyes compared with the unmodified AuNPs, and the absorbance

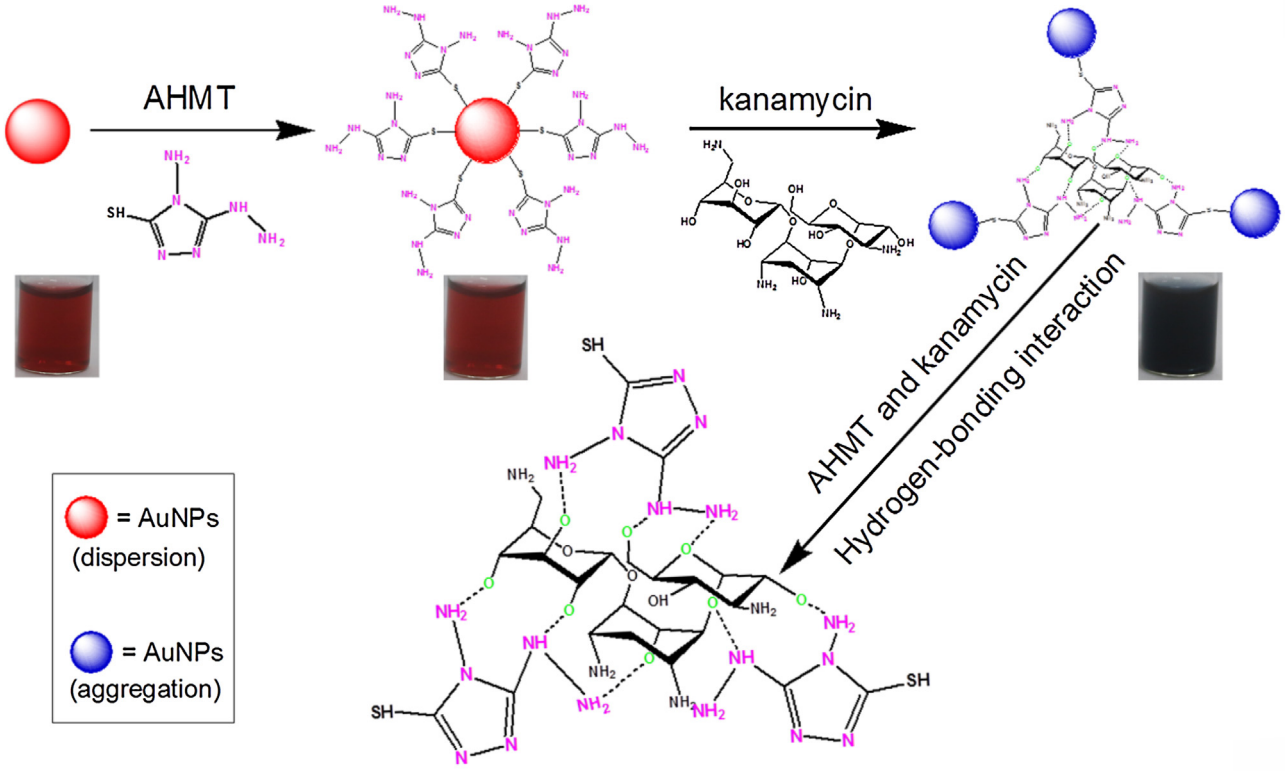

Scheme 1. Colorimetric detection of kanamycin using the AHMT-functionalized gold nanoparticles based on the hydrogen-bonding interaction.

at 520 nm of UV–vis absorption spectra slightly decreased. It is possible because that AHMT could result in the part aggregation of AuNPs since it has mercapto group and N atom, which was demonstrated by the following experiment and it indicated the combination of AHMT and AuNPs. In addition, the incubation time was much longer than the reaction time resulting in a constant absorbance that verified the existence of AHMT with the concentration of 0.05 mM had no influence on the results and the stability of AuNPs. Moreover, when the amount of KA added into the AHMT-AuNPs solution, the color changed from wine red to deep purple rapidly and the intensity of the spectral feature at 650 nm was seen to increase, while the signal observed at 520 nm decreased and became broader accordingly (Fig. 1). It indicated that KA was combined with AHMT on the surface of AuNPs, decreased the distance and led to a shift of the surface plasma resonance peak and a red-to-purple color change (Fig. 1, inset). TEM images (Fig. 2) also proved the aggregation of AHMT-AuNPs. Fig. 2 showed the TEM images of AHMT-AuNPs in the absence (Fig. 2B) and presence (Fig. 2C) of 5 μM KA. In the absence and presence of AHMT, AuNPs were both well dispersed (Fig. 2A and B). On the other hand, apparent aggregation occurs when KA was added (Fig. 2C). What's more, it is reported that most of KA could be triprotonated and formed three positive charges at pH 6.7, which adsorbed on the surface of AuNPs and led to aggregation. The —OH groups of KA could serve as the bridge to form intermolecular hydrogen bonds and expand the AuNPs aggregation [24]. Hence, the color changed and UV–vis absorption spectra of AuNPs adding with KA alone were also recorded. It is true that KA could cause the aggregation of AuNPs, but what is noteworthy is that the color was not so deep when compared with the color of AHMT-AuNPs system and the UV–vis absorption spectra proved this phenomenon in Fig. 1. It may attribute to the intensity of Au-S bond is stronger than the Au-N bond and the KA may disperse in solution after thorough stirring [37,38]. At the same time, when KA is coexisted with AHMT, the spatial hindrance induced by the hydrogen-bonding interaction between KA and AHMT might allow the mercapto group of the AHMT binding onto the surface of AuNPs only, instead of the nitrogens from the hybrid ring and the exocyclic amino groups (Scheme 1). On the other hand, to validate the hydrogen-bonding interaction of KA and AHMT, the zeta potential of AHMT-AuNPs solution with different concentrations of KA (KA-AHMT-AuNPs) was measured. As exhibited in Fig. S-1, with the increasing concentration of KA, the potential of AHMT-AuNPs increased gradually, which indicates the reducing of negative charge, increase of positive charge and aggregation of AHMT-AuNPs. Thus, the results illustrate that the AHMT-AuNPs are sensitively responded to KA by hydrogen-bonding interaction.

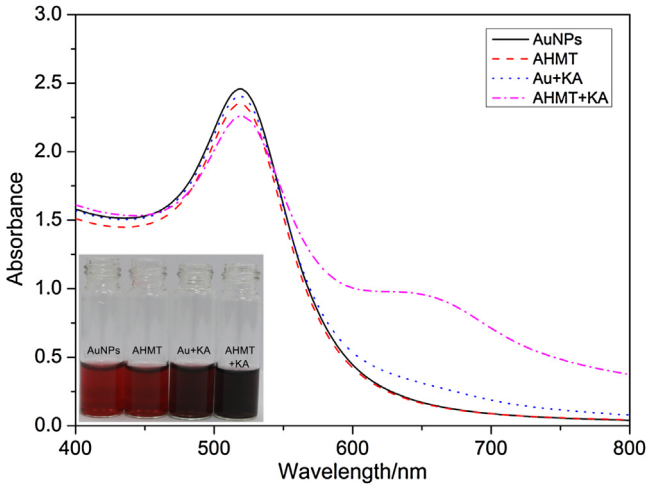

Fig. 1. UV–vis absorption spectra of the AuNPs, AHMT-AuNPs, AuNPs in the presence of 5 μM kanamycin and AHMT-AuNPs in the presence of 5 μM kanamycin at pH 7.4 in room temperature. Inset shows the color change versus the AuNPs, AHMT-AuNPs, AuNPs in the presence of 5 μM kanamycin and AHMT-AuNPs in the presence of 5 μM kanamycin at pH value of 7.4 in room temperature.

3.2. Optimal concentration of AHMT

The colorimetric determination of KA was strongly influenced by the experimental conditions, such as the concentration of AHMT, media pH, reaction time and temperature. For this, different conditions were investigated in this work.

For the optimum concentration of AHMT, six different concentrations, 10, 50, 75, 100, 500, and 1000 μM, were diluted respectively. For the best sensitivity, the AHMT-AuNPs solutions obtained at pH 7.4 in room temperature. With the increase of the concentration, the color change of AHMT-AuNPs was observed gradually from red to purple (Fig. S-2 inset) when the concentration was above 100 μM. In addition, when the concentration exceeded 75 μM, a marked increase in the spectral feature at longer wavelength and decreased at 520 nm was exhibited. But it was different with the KA-AHMT-AuNPs system, which showed another peak at 650 nm (Fig. S-2). It is because that the mercapto group of AHMT can bind with the AuNPs on the surface. Furthermore, the exocyclic amino groups and three nitrogen hybrid ring of AHMT lead to the combination of AHMT and AuNPs either, so the color changed from red-to-purple. But the N-Au bond is not so stronger than the S-Au, which was not enough for the aggregation to form another peak at 650 nm. In consideration of the response sensitivity and background signal, 50 μM AHMT was selected as the optimized concentration.

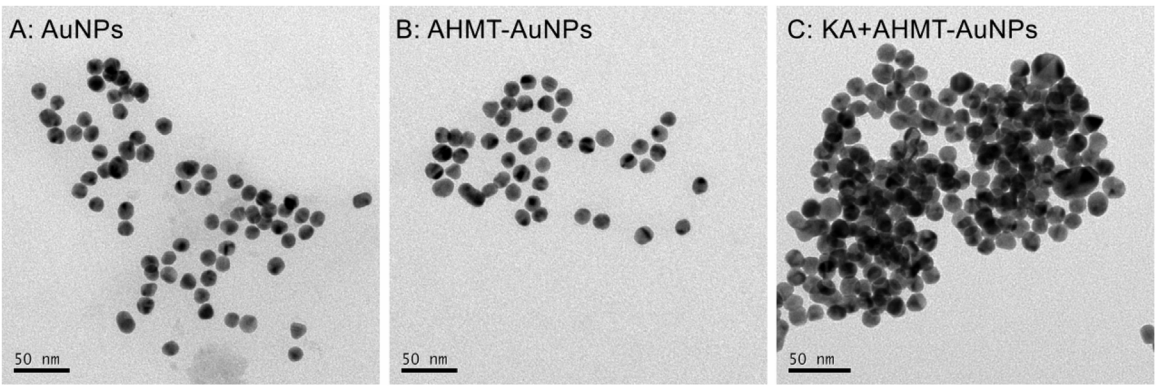

Fig. 2. Transmission electron microscope images of the (A) AuNPs, (B) AHMT-AuNPs, and (C) AHMT-AuNPs in the presence of 5 μM kanamycin.

3.3. Temperature and pH effects

AHMT-AuNPs were synthesized at room temperature, and the sensitivity of AHMT- AuNPs system to KA at different temperature (10, 15, 20, 25, 30, 35, 40, 45, 50, 55, 60, 65, 70 °C) was investigated by setting the AuNPs solutions to the water bath and refrigerator, respectively. The KA added, and the UV–vis absorption spectra were measured after the reaction of 10 min. The level of AHMT-AuNPs aggregation was demonstrated by the ratio absorbance of the UV–vis absorption spectra at 650 nm and 520 nm (A_{650}/A_{520}). After the addition of KA, with the increase of temperature to 25 °C, the ratio of A_{650}/A_{520} was also increased slightly, and then it declined very slowly (Fig. S-3A). When the temperature reached 70 °C, the ratio of A_{650}/A_{520} decreased sharply. That may be because that the structure and property of KA or AHMT changed in such high temperature. Meanwhile, the UV–vis absorption spectra of the AHMT-AuNPs with different temperatures (15, 25, and 35 °C) in the presence of 5, 10, and 100 μM kanamycin at pH 7.4 were detected (Fig. S-3A–D) and the results showed the AHMT-AuNPs system was not so sensitive to the temperature. It can be used as a colorimetric sensor for KA in a broad temperature range and is convenient for real-time application. Hence, the whole process of experiment was set at the room temperature.

Owing to the reaction process related with hydrogen-bonding interaction, which is strongly influenced by H^+, the pH was a key factor for the sensitivity of AHMT-AuNPs system. It has been reported that due to the repulsive electrostatic forces of AuNPs at lower or higher pH, the optimum pH should be determined for each aggregation [39]. In their study, the aggregation rate peaks were at pH 7.0 because of the repulsive electrostatic forces at higher or lower pH. Results reported by Xiao et al. [40] have shown that under the near-neutral pH conditions, the melamine was more easily absorbed onto the AuNPs surface. Herein, different pH in the range of 6.4-8.0 was investigated in this work (Fig. S-4). It is clear that the effects of pH in such range are not so obvious, which means the AHMT-AuNPs system is helpful in relative broad range. With the increasing from 6.4 to 7.4, the ratio of A_{650}/A_{520} also increased, while started decreasing when the pH above 7.4. It can be seen that the AHMT-AuNPs system presents better sensitivity in the detection of KA (5 μM) in pH 7.4, in which the maximal ratio of A_{650}/A_{520} indicated. So, pH 7.4 was regarded as the ideal conditions for the measurement of KA. The results are essentially consistent with the reported study [27,36].

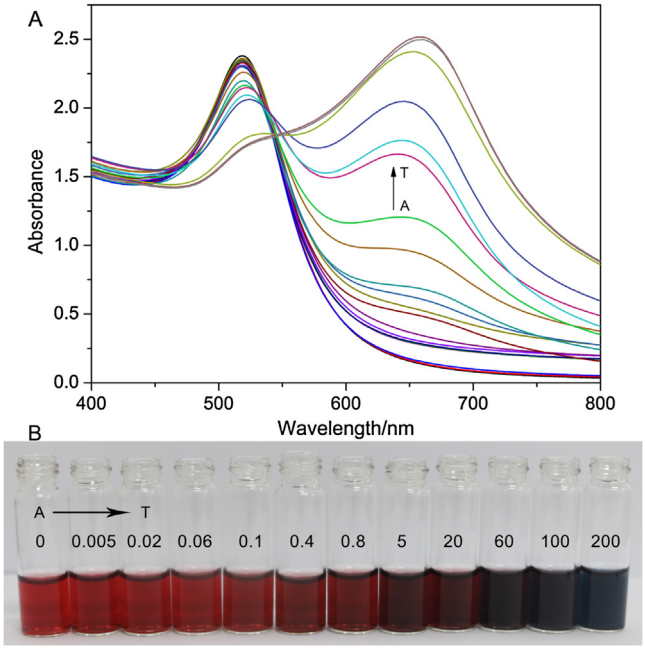

Fig. 3. (A) UV–vis absorption spectra of AHMT-AuNPs in the presence of different concentrations of kanamycin at pH 7.4 in room temperature (A to T express 0, 0.005, 0.01, 0.02, 0.04, 0.06, 0.08, 0.1, 0.2, 0.4, 0.8, 1, 5, 10, 20, 40, 60, 100,150, 200 μM, respectively). (B) Color changes of the images for AHMT-AuNPs containing different concentrations of kanamycin at pH 7.4 in room temperature (0, 0.005, 0.02, 0.06, 0.1, 0.4, 0.8, 5, 20, 60, 100, 200 μM, respectively).

3.4. The optimum of reaction time

As expected, incubation time and reaction time also influence the colorimetric responses of the AHMT-AuNPs system in the presence of KA. The incubation time of AHMT adsorbed on the surface of AuNPs was 2 h according to the reported literature [29]. With respect to the reaction time, it was shown that the color changed from deep red to purple and blue, and the absorbance peak decreased gradually at 520 nm when extending the reaction time in the experimental process. Meanwhile, another shoulder peak emerged at 650 nm, then, slowly red shifted and became stronger in 10 min. As exhibited in Fig. S-5, four different concentrations (0.1, 5, 40, 100 μM) of KA were added to the AHMT-AuNPs solution, and the absorption spectra was recorded continuously in 25 min. As a result, the absorption ratio of A_{650}/A_{520} quickly increased within 10 min, whereas a plateau was reached when the time was more than 10 min. Thus, 10 min were chosen for the optimal reaction time in the experiments.

3.5. Sensitive colorimetric detection of KA

In order to verify the visual colorimetric detection of KA, UV–vis spectra were recorded in the absence and presence of different concentrations of KA. It is well known that the color of citrate-stabilized AuNPs was wine red, and exhibited a property absorption band at 520 nm. However, upon the addition of different concentrations (from 0.005 to 200 μM) of KA combining with AHMT, a series of color change from red to purple and blue turned up and a significant change in the spectral profile were observed (Fig. 3). These changes are as follows: (1) a gradual decreasing for the peak of the absorption spectra at 520 nm, (2) the appearance of a new band at 650 nm, (3) obvious red shift and increasing of the absorption spectra at 650 nm (Fig. 3A), which showed the aggregation of AuNPs. Most importantly, even the addition of trace amounts of KA could result in a significant color change, which could be distinguished by the naked eye, provided a visual application of AuNPs. Direct evidence for KA-stimulated aggregation of AHMT-AuNPs could be further proved by the transmission electron microscopy (TEM) images (Fig. 2). In addition, quantitative analysis was investigated via adding different concentrations of KA to AHMT–AuNPs and monitored through UV–vis absorption spectra. The ratio of A_{650}/A_{520} has been used to represent the aggregating degree of AuNPs and quantify the concentration of KA. As shown in Fig. 4A, it was found that the ratio increased gradually with the rising concentration of KA. Moreover, under the optimum condition, two linear correlations exhibited in the range from 0.005 to 0.1 μM and from 0.1 to 20 μM, with the correlation coefficients of 0.9936 (Fig. 4B) and 0.9867 (Fig. 4C), respectively. The calibration equation was obtained by fitting the experimental data:

$$y = (0.7749 \pm 0.012)x + (0.0795 \pm 0.023) \quad (1)$$

$$y = (0.0321 \pm 0.0042)x + (0.2148 \pm 0.034) \quad (2)$$

Where y is the absorption ratio of A_{650}/A_{520}, and x is the concentration of KA (μM). Additionally, the correlation coefficient of the equation is 0.9936 and 0.9867, respectively. Furthermore, the

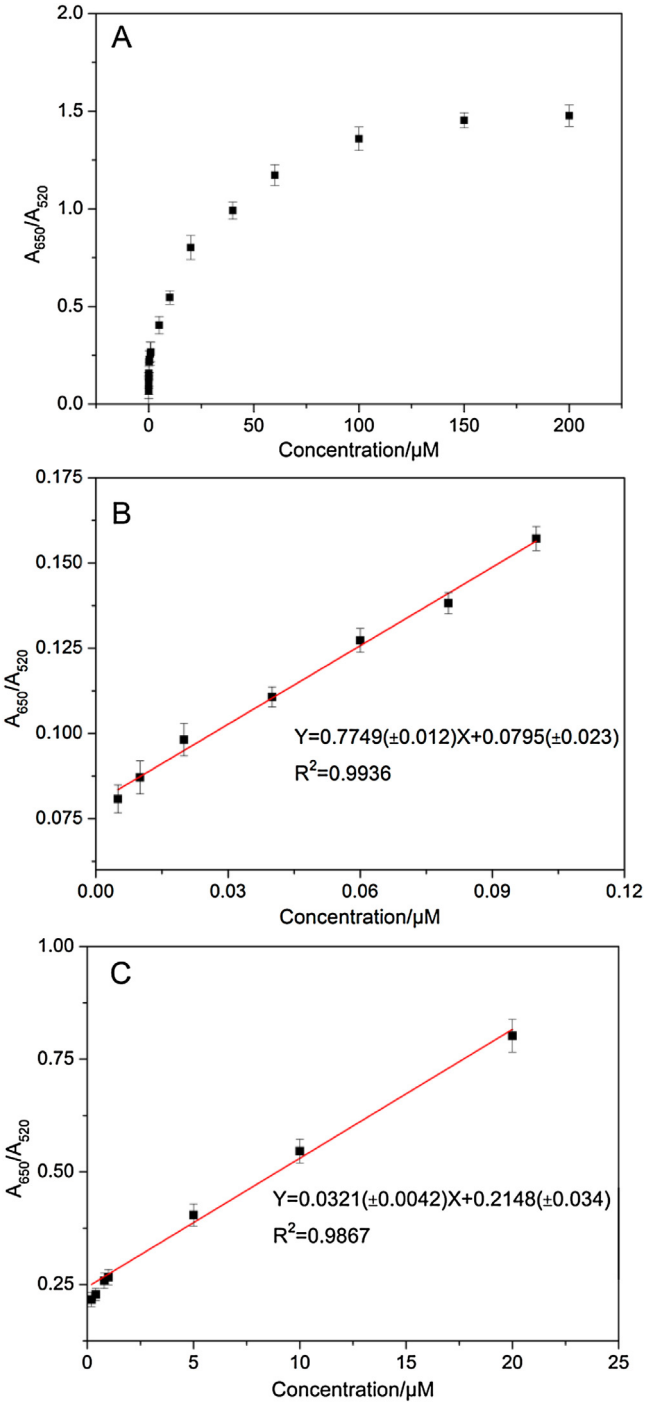

Fig. 4. (A) The absorption ratio (A_{650}/A_{520}) of AHMT-AuNPs versus different concentrations of kanamycin at pH 7.4 in room temperature (0, 0.005, 0.01, 0.02, 0.04, 0.06, 0.08, 0.1, 0.2, 0.4, 0.8, 1, 5, 10, 20, 40, 60, 100,150, 200 μM, respectively). Error bars were obtained from three experiments. (B) The linear correlation of the absorption ratio (A_{650}/A_{520}) for AHMT-AuNPs in the range of 0.005–0.1 μM. (C) The linear correlation of the absorption ratio (A_{650}/A_{520}) for AHMT-AuNPs in the range of 0.1–20 μM. Error bars were obtained from three experiments.

detection limit (LOD) is calculated according to the following formula:

$$LOD = 3.3(SD/S) \quad (3)$$

Where SD is the standard deviation of the response of blank, and S is the slope of the calibration curves [41]. Since, the LOD of 0.004 μM (S/N = 3) based on this approach could be obtained, which is much lower than the MAL (maximum allowable level) of ~0.25 μM (146 ppb) in milk defined by the European Union [19,42]. In the existence of high concentration of KA, the UV–vis absorption spectra became much broader and the red shift observed, the A_{650}/A_{520} value was not in a linear range. That may be because the concentration of AHMT-AuNPs was close to saturation. It is similar to most of this kind of researches [37,43,44]. Comparing with other sensors (Table 1), the sensitivity of this method is also satisfactory.

3.6. Selectivity and interference study of KA

For investigating the selectivity of this system to KA, some common potentially interfering substances were added into the AHMT-AuNPs solution, with the same concentrations of 20 μM, which was much higher than the concentration of 5 μM for KA. The extinction ratio (A_{650}/A_{520}) response in the presence of other molecules with similar structures was monitored to evaluate the selectivity of the optimized sensor for KA. The results showed high selectivity for KA over Tetracycline, L-arginine, L-aspartic acid, Glucose, Glutathione, Glycine, L-cysteine, and L-phenylalanine (Fig. 5). Meanwhile, in contrast to the significant response observed for KA, negligible signal changes were observed upon the addition of some metal ions. As exhibited in Fig. S-6, the color changes of AHMT-AuNPs induced by the addition of similar substances and metal ions were obtained. Except KA, few of these chemicals could lead to the red-to-blue color change, which showed good selectivity toward KA because of the hydrogen-bonding interaction between KA and AHMT. Moreover, KA and other chemicals including the amino acid and metal ions were mixed to form a mixture solution as a sample for the interference study of this sensor. The extinction ratio (A_{650}/A_{520}) response was obviously higher than other samples without KA. These results indicated that this sensor was not only insensitive to other substances but also selective toward KA in their presence. As mentioned above, the present sensor has outstanding anti-interference capability and satisfactory selectivity.

3.7. Real samples detection

To evaluate the practical application of the proposed method, several real samples spiked with KA including environmental water samples, milk samples, and urine samples, with concentrations of 0.01, 1.0, and 5.0 μM, were tested using the proposed method and HPLC. The environmental water samples used in this work were tap water, drinking water, river water, and pond water samples. Through measuring, the sole addition of these samples to the AHMT-AuNPs solution did not lead to a distinguish color change. However, when the samples with 0.01, 1.0, and 5.0 μM KA were added, a red-to-purple color change could be observed clearly, coinciding with the extinction ratio (A_{650}/A_{520}) response. As shown in Table 2, the concentration of KA in the spiked water samples detected by the AHMT-AuNPs system with an external calibration revealed good agreement with the measurement of HPLC. More importantly, such a colorimetric sensor also can find potential application in the detection of KA in milk and urine. Similarly, when the three concentrations of KA (0.01, 1.0, and 5.0 μM) added, a red-to-purple color change could be observed, and the extinction ratio (A_{650}/A_{520}) response agreed with the results (Table 3). It could be seen that there was little interference encountered in the analysis of these samples.

4. Conclusions

In summary, a simple, reliable and sensitive detecting method in various samples based on the hydrogen-bonding interaction of AHMT functionalized gold nanoparticles was developed for the highly sensitive detection of kanamycin. The AHMT functionalized

Table 1
Comparison of different methods for the detection of kanamycin.

Technique	Supporting	Linear range (nM)	LOD (nM)	References
Colorimetry	PRLS[a]	20–800	2	[1]
	DNA[b] aptamer	Not shown	25	[2]
	Pyrocatechol violet (PCV)	10–500 and 500–55000	1	[3]
	AHMT	5–100 and 100–20000	4	This work
Electrochemical	[c]Poly-DPB aptamer (CVs and LSV)	50–9000	9.47 ± 0.4	[4]
detection	aptamer	0.1–60	0.06	[5]
[d]MRS immunosensor	[e]B-SA system	2.6–43	0.17	[6]
Electrochemical immunosensor	([f]WGS)/[g]PB-CTS/[h]NPG	34–24000	10.83	[7]
immunosensor	Ag@Fe3O4 NPs and [i]TH-GS	86–27000	25.75	[8]
Fluorescence	ssDNA aptamer	1–100	1.49	[9]
	aptamer	0.8–350	0.3	[10]
	exonuclease III and aptamer	0.5–20	0.321	[11]

[a] PRLS, plasmon resonance light scattering.
[b] DNA, Ky2 aptamer.
[c] poly-DPB, TGGGGGTTGAGGCTAAGCCGAC.
[d] MRS, magnetic relaxation switch.
[e] B-SA, biotin-streptavidin.
[f] WGS, water-soluble grapheme sheet.
[g] PB-CTS, prussian blue-chitosan.
[h] NPG, nanoporous gold.
[i] TH-GS, thionine mixed graphene sheet.

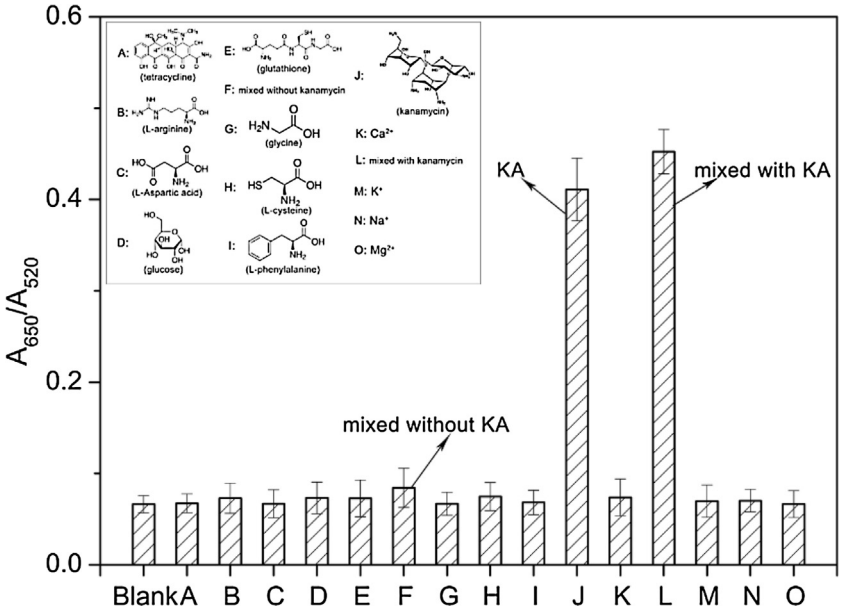

Fig. 5. The absorption ratio (A_{650}/A_{520}) of AHMT-AuNPs versus different kinds of similar substances and metal ions (20 μM) at pH 7.4 in room temperature (A to O express the Tetracycline, L-arginine, L-aspartic acid, Glucose, Glutathione, mixed without kanamycin, Glycine, L-cysteine, L-phenylalanine, kanamycin, Ca^{2+}, mixed with kanamycin, K^+, Na^+, and Mg^{2+}, respectively). The concentration of kanamycin was 5 μM while those of the other chemicals were 20 μM. Error bars were obtained from three experiments.

Table 2
Levels of kanamycin in real water samples were measured using our method and HPLC measurement with the range of Relative Standard Deviation from 0.203% to 1.98%.

Samples	Added (μM)	Found (μM)	Recovery (%)	RSD[a] (%)	HPLC[b] (μM)
Tap water	0.01	0.011	110.00	0.293	0.012
	1	1.022	102.20	0.352	1.021
	5	4.962	99.24	1.036	5.022
Drinking water	0.01	0.012	120.00	0.243	0.010
	1	0.982	98.20	0.735	1.002
	5	5.030	100.60	1.748	5.021
River water	0.01	0.012	120.00	0.272	0.010
	1	1.068	106.80	0.731	1.002
	5	5.442	108.84	1.463	5.032
Pond water	0.01	0.011	110.00	0.203	0.011
	1	1.073	107.30	1.524	1.023
	5	5.084	101.68	1.980	5.051

[a] RSD, relative standard deviation.
[b] HPLC, High performance liquid chromatography.

Table 3
Levels of kanamycin in real samples of milk and urine were measured using our method and the HPLC measurement with the range of Relative Standard Deviation from 0.264% to 1.427%.

Samples	Added (μM)	Found (μM)	Recovery (%)	RSD[a] (%)	HPLC[b] (μM)
Milk	0.01	0.012	120.00	0.374	0.011
	1	1.041	104.10	0.643	1.010
	5	5.067	101.34	1.216	5.034
Urine	0.01	0.011	110.00	0.264	0.010
	1	1.023	102.30	0.845	1.008
	5	5.053	101.06	1.427	5.036

[a] RSD, relative standard deviation.
[b] HPLC, High performance liquid chromatography.

gold nanoparticles were aggregated owing to the hydrogen-bonding interaction between KA and AHMT. The concentration of KA can be determined with a UV–vis spectrometer and the naked eyes, which provided a visual method. The interference chemicals including common amine acid and antibiotics or metal ions did not affect the detection of KA. The novel method provides several advantages over current KA detection techniques. Firstly, this approach does not require complicated or expensive instruments, which reduces the cost and simplifies operations. Secondly, the approach allows a determination concentration as low as 0.004 μM, useful for ultrasensitive and rapid detection of KA in various real samples. Particularly, the proposed method can be successfully applied to the determination of KA in various real samples with high reveries from 98.2% to 120%. Finally, this sensor shows excellent selectivity for KA over other molecules. These advantages substantially allow this approach quite promising for simple and real-time determination of KA in water samples, milk, and urine, as well as other real samples. This study reveals a promising application of gold nanoparticles in organic molecules detection. Further studies on more application of gold nanoparticles are needed to develop in the future.

Acknowledgments

This study was financially supported by the National Natural Science Foundation of China (51278176, 51378190, 51408206, 51521006, 51579096, and 51579098), the National Program for Support of Top–Notch Young Professionals of China (2014), the Program for Changjiang Scholars and Innovative Research Team in University (IRT-13R17), the Fundamental Research Funds for the Central Universities, the Program for New Century Excellent Talents in University (NCET-13-0186), Scientific Research Fund of Hunan Provincial Education Department (No.521293050), the Hunan Provincial Innovation Foundation for Postgraduate (CX2015B091) and the Hunan Provincial Natural Science Foundation of China (2015JJ2031).

Appendix A. Supplementary data

Supplementary data associated with this article can be found, in the online version, at http://dx.doi.org/10.1016/j.snb.2016.12.086.

References

[1] S. Saha, P. Sarkar, A.P. Turner, Interference-free electrochemical detection of nanomolar dopamine using doped polypyrrole and silver nanoparticles, Electroanalysis 26 (2014) 2197–2206.
[2] M. Turner, V.B. Golovko, O.P. Vaughan, P. Abdulkin, A. Berenguer-Murcia, M.S. Tikhov, et al., Selective oxidation with dioxygen by gold nanoparticle catalysts derived from 55-atom clusters, Nature 454 (2008) 981–983.
[3] K. Saha, S.S. Agasti, C. Kim, X. Li, V.M. Rotello, Gold nanoparticles in chemical and biological sensing, Chem. Rev. 112 (2012) 2739–2779.
[4] G. Zeng, C. Zhang, D. Huang, C. Lai, L. Tang, Y. Zhou, et al., Practical and regenerable electrochemical aptasensor based on nanoporous gold and thymine-Hg $^{2+}$-thymine base pairs for Hg $^{2+}$ detection, Biosens. Bioelectron. (2016).
[5] C. Zhang, C. Lai, G. Zeng, D. Huang, L. Tang, C. Yang, et al., Nanoporous Au-based chronocoulometric aptasensor for amplified detection of Pb(2+) using DNAzyme modified with Au nanoparticles, Biosens. Bioelectron. 81 (2016) 61–67.
[6] S. Wu, D. Li, J. Wang, Y. Zhao, S. Dong, X. Wang, Gold nanoparticles dissolution based colorimetric method for highly sensitive detection of organophosphate pesticides, Sens. Actuators B 238 (2017) 427–433.
[7] L.-p. Zhang, Y.-p. Xing, L.-h. Liu, X.-h. Zhou, H.-c. Shi, Fenton reaction-triggered colorimetric detection of phenols in water samples using unmodified gold nanoparticles, Sens. Actuators B 225 (2016) 593–599.
[8] R. Elghanian, J.J. Storhoff, R.C. Mucic, R.L. Letsinger, C.A. Mirkin, Selective colorimetric detection of polynucleotides based on the distance-dependent optical properties of gold nanoparticles, Science 277 (1997) 1078–1081.
[9] Y. Guo, Z. Wang, W. Qu, H. Shao, X. Jiang, Colorimetric detection of mercury, lead and copper ions simultaneously using protein-functionalized gold nanoparticles, Biosens. Bioelectron. 26 (2011) 4064–4069.
[10] C. Lai, Q. Lei, Z. Guangming, L. Yunguo, H. Danlian, Z. Chen, et al., Sensitive and selective detection of mercury ions based on papain and 2,6-pyridinedicarboxylic acid functionalized gold nanoparticles, Rsc. Adv. 6 (2015) 3259–3266.
[11] X. Zhang, H. Zhao, Y. Xue, Z. Wu, Y. Zhang, Y. He, et al., Colorimetric sensing of clenbuterol using gold nanoparticles in the presence of melamine, Biosens. Bioelectron. 34 (2012) 112–117.
[12] Y. Zhou, P. Wang, X. Su, H. Zhao, Y. He, Colorimetric detection of ractopamine and salbutamol using gold nanoparticles functionalized with melamine as a probe, Talanta 112 (2013) 20–25.
[13] E. Arunan, G.R. Desiraju, R.A. Klein, J. Sadlej, S. Scheiner, I. Alkorta, et al., Defining the hydrogen bond: an account (IUPAC technical report), Pure Appl. Chem. 83 (2011) 1619–1636.
[14] K. Ai, Y. Liu, L. Lu, Hydrogen-bonding recognition-induced color change of gold nanoparticles for visual detection of melamine in raw milk and infant formula, J. Am. Chem. Soc. 131 (2009) 9496–9497.
[15] C. Zhang, C. Lai, G. Zeng, D. Huang, C. Yang, Y. Wang, et al., Efficacy of carbonaceous nanocomposites for sorbing ionizable antibiotic sulfamethazine from aqueous solution, Water Res. 95 (2016) 103–112.
[16] Y.H. Long, M. Hernandez, E. Kaale, A. Van Schepdael, E. Roets, F. Borrull, et al., Determination of kanamycin in serum by solid-phase extraction, pre-capillary derivatization and capillary electrophoresis, J. Chromatogr. B 784 (2003) 255–264.
[17] G. Zeng, M. Chen, Z. Zeng, Risks of neonicotinoid pesticides, Science 340 (2013) 1403.
[18] N.C. Megoulas, M.A. Koupparis, Direct determination of kanamycin in raw materials, veterinary formulation and culture media using a novel liquid chromatography–evaporative light scattering method, Anal. Chim. Acta 547 (2005) 64–72.
[19] S. Yu, Q. Wei, B. Du, D. Wu, H. Li, L. Yan, et al., Label-free immunosensor for the detection of kanamycin using Ag@Fe(3)O(4) nanoparticles and thionine mixed graphene sheet, Biosens. Bioelectron. 48 (2013) 224–229.
[20] S.H. Chen, Y.C. Liang, Y.W. Chou, Analysis of kanamycin A in human plasma and in oral dosage form by derivatization with 1-naphthyl isothiocyanate and high-performance liquid chromatography, J. Sep. Sci. 29 (2006) 607–612.
[21] Y.X. Zhou, W.J. Yang, L.Y. Zhang, Z.Y. Wang, Determination of kanamycin A in animal feeds by solid phase extraction and high performance liquid chromatography with pre-column derivatization and fluorescence detection, J. Liq. Chromatogr. Relat. Technol. 30 (2007) 1603–1615.
[22] Y.P. Chen, M. Zou, C. Qi, M.X. Xie, D.N. Wang, Y.F. Wang, et al., Immunosensor based on magnetic relaxation switch and biotin-streptavidin system for the detection of Kanamycin in milk, Biosens. Bioelectron. 39 (2013) 112–117.
[23] B.Y. Zhao, Q. Wei, C. Xu, H. Li, D. Wu, Y. Cai, et al., Label-free electrochemical immunosensor for sensitive detection of kanamycin, Sens. Actuators B 155 (2011) 618–625.
[24] X. Wang, M. Zou, X. Xu, R. Lei, K. Li, N. Li, Determination of human urinary kanamycin in one step using urea-enhanced surface plasmon resonance light-scattering of gold nanoparticles, Anal. Bioanal. Chem. 395 (2009) 2397–2403.
[25] K.M. Song, M. Cho, H. Jo, K. Min, S.H. Jeon, T. Kim, et al., Gold nanoparticle-based colorimetric detection of kanamycin using a DNA aptamer, Anal. Biochem. 415 (2011) 175–181.

[26] M. Preu, D. Guyot, M. Petz, Development of a gas chromatography–mass spectrometry method for the analysis of aminoglycoside antibiotics using experimental design for the optimisation of the derivatisation reactions, J. Chromatogr. A 818 (1998) 95–108.
[27] J.J. Feng, H. Guo, Y.F. Li, Y.H. Wang, W.Y. Chen, A.J. Wang, Single molecular functionalized gold nanoparticles for hydrogen-bonding recognition and colorimetric detection of dopamine with high sensitivity and selectivity, ACS Appl. Mater. Interfaces 5 (2013) 1226–1231.
[28] L. Wang, C.L. Zhou, H.Q. Chen, J.G. Chen, J. Fu, B. Ling, Determination of formaldehyde in aqueous solutions by a novel fluorescence energy transfer system, Analyst 135 (2010) 2139–2143.
[29] A.J. Wang, H. Guo, M. Zhang, D.L. Zhou, R.Z. Wang, J.J. Feng, Sensitive and selective colorimetric detection of cadmium(II) using gold nanoparticles modified with 4-amino-3-hydrazino-5-mercapto-1,2,4-triazole, Microchim. Acta 180 (2013) 1051–1057.
[30] D.C. Sherrington, K.A. Taskinen, Self-assembly in synthetic macromolecular systems via multiple hydrogen bonding interactions, Chem. Soc. Rev. 30 (2001) 83–93.
[31] C. Zhang, L. Liu, G.-M. Zeng, D.-L. Huang, C. Lai, C. Huang, et al., Utilization of nano-gold tracing technique: study the adsorption and transmission of laccase in mediator-involved enzymatic degradation of lignin during solid-state fermentation, Biochem. Eng. J. 91 (2014) 149–156.
[32] C.C. Huang, H.T. Chang, Parameters for selective colorimetric sensing of mercury(II) in aqueous solutions using mercaptopropionic acid-modified gold nanoparticles, Chem. Commun. (Camb.) (2007) 1215–1217.
[33] C. Pezzato, S. Maiti, J.L. Chen, A. Cazzolaro, C. Gobbo, L.J. Prins, Monolayer protected gold nanoparticles with metal-ion binding sites: functional systems for chemosensing applications, Chem. Commun. (Camb.) 51 (2015) 9922–9931.
[34] S. Manna, A. Saha, A.K. Nandi, A two component thermoreversible hydrogel of riboflavin and melamine: enhancement of photoluminescence in the gel form, Chem. Commun. (2006) 4285–4287.
[35] J.J. Feng, H. Guo, Y.F. Li, Y.H. Wang, W.Y. Chen, A.J. Wang, Single molecular functionalized gold nanoparticles for hydrogen-bonding recognition and colorimetric detection of dopamine with high sensitivity and selectivity, ACS Appl. Mater. Interfaces 5 (2013) 1226–1231.
[36] Z. Chen, Y. Hu, Q. Yang, C. Wan, Y. Tan, H. Ma, A highly sensitive colorimetric sensor for adrenaline detection based on organic molecules-functionalized gold nanoparticles, Sens. Actuators B 207 (2015) 277–280.
[37] Y.-L. Li, Y.-M. Leng, Y.-J. Zhang, T.-H. Li, Z.-Y. Shen, A.-G. Wu, A new simple and reliable Hg^{2+} detection system based on anti-aggregation of unmodified gold nanoparticles in the presence of O-phenylenediamine, Sens. Actuators B 200 (2014) 140–146.
[38] R. Wilson, The use of gold nanoparticles in diagnostics and detection, Chem. Soc. Rev 37 (2008) 2028–2045.
[39] N.T.K. Thanh, Z. Rosenzweig, A. Chem, Development of an aggregation-based immunoassay for anti-protein a using gold nanoparticles, Anal. Chem 74 (2002) 1624–1628.
[40] C. Xiao, J. Liu, A. Yang, H. Zhao, Y. He, X. Li, et al., Colorimetric determination of neomycin using melamine modified gold nanoparticles, Microchim. Acta 182 (2015) 1501–1507.
[41] G.A. Shabir, Validation of high-performance liquid chromatography methods for pharmaceutical analysis: understanding the differences and similarities between validation requirements of the US Food and Drug Administration, the US Pharmacopeia and the International Conference on Harmonization, J. Chromatogr. A 987 (2003) 57–66.
[42] B.Y. Zhao, Q. Wei, C. Xu, H. Li, D. Wu, Y. Cai, et al., Label-free electrochemical immunosensor for sensitive detection of kanamycin, Sens. Actuators B 155 (2011) 618–625.
[43] Z. Chen, C. Zhang, T. Zhou, H. Ma, Gold nanoparticle based colorimetric probe for dopamine detection based on the interaction between dopamine and melamine, Microchim. Acta 182 (2014) 1003–1008.
[44] X. Xu, J. Wang, K. Jiao, X. Yang, Colorimetric detection of mercury ion (Hg^{2+}) based on DNA oligonucleotides and unmodified gold nanoparticles sensing system with a tunable detection range, Biosens. Bioelectron. 24 (2009) 3153–3158.

Biographies

Lei Qin received her B.S. degree in Environmental Engineering in University of South China, Hengyang, China. She is currently in the first year of her PhD in Hunan University under the supervision of Prof. Guangming Zeng. Her current research interests focus on the fabrication and application of nano materials in environmental detection and control.

Prof. Guangming Zeng teaches courses and performs research on the remediation of polluted soils and solubilization of organic pollutants by surfactants at Hunan University since 1988. He has been head of the School of Environmental Science and Engineering since 1996 at the same University. His honors include the National Science and Technology Progress Awards of China (the Second Award), National Technology Invention Awards of China (the Second Award), and a Lifetime Achievement Award of Changjiang Scholars. He participated to the supervision of 120 PhD and 270 MSc. Prof. Zeng has published more than 500 peer-reviewed papers with more than 13000 citations and H factor 57 (according to ISI web of Science).

Cui Lai graduated from the College of Environmental Science and Engineering of Hunan University in 2013 and received her PhD degree in Environmental Science. She joined Professor Guangming Zeng's group at Hunan University after completing her PhD degree. Her main research interests are the development and environmental application of functional nanomaterials.

Prof. Danlian Huang obtained her PhD in Environmental Engineering in Hunan University in 2011. In 2015 she was promoted to Full Professor of Environmental Engineering at the same University. Her research has focused on the remediation of soils polluted by organic compounds and heavy metals. Prof. Huang has co-authored over 90 papers in peer-reviewed international journals. Her honors include the New Century Excellent Talents in University, the Science and Technology Progress Award of Hunan Province (the First Award).

Chen Zhang has nearly finished his PhD studies in key laboratory of environment biology and pollution control, Hunan University, working under the supervision of Prof. Guangming Zeng. His research interests focus on the fabrication of nano materials and their applications in pollutant detection and control.

Piao Xu received her PhD degree in college of Environmental Science and Engineering, Hunan University in 2016. She is currently a post-doctoral researcher in College of materials science and engineering, Hunan University. Her major research focus is on the development of iron oxide nanomaterials and application in environmental remediation.

Dr. Tianjue Hu teaches courses and performs research on the Application of microorganism in environment engineering and Management and disposition of organic solid waste at Hunan University since 1997. He teaches two curriculums: Environment Engineering Principle and Environment Engineering CAD. His honors include the National Science and Technology Progress Awards of China (the Second Award, 2006), the Hunan Province Science and Technology Progress Award (the First Award, 2003). He has published more than 40 papers and two works.

Xigui Liu received his B.S. degree in the college of Resources and Environment, Jinan University in 2014. He is currently a Master degree candidate in college of Environmental Science and Engineering, Hunan University. He is studying in research groups of Professor Guangmin Zeng and assistant Professor Cui Lai. His major research is focus on the development of AuNPs and application in detection, as well as electrochemical detection.

Min Cheng received his MSc in 2014 in Environmental Engineering in Hunan University, Changsha, China. He is currently in the second year of his PhD in Hunan University under the supervision of Prof. Guangming Zeng. His current research focus on the remediation of hydrophobic organic compounds polluted soils with particular interest in the development of cost-effective and ecologically sound surfactants-based techniques. He has published over 20 papers in peer-reviewed international journals. Min Cheng was awarded the Excellent Graduation Thesis for Master Degree of Hunan Province in 2014.

Yang Liu received her MSc in 2014 in Environmental Engineering in Hunan University, Changsha, China. She is currently in the third year of her PhD in Hunan University under the supervision of Prof. Guangming Zeng. Her current research focus on the bioremediation of hydrophobic organic compounds contaminated environment with particular interest in the development of cost-effective and ecologically sound biosurfactant-based techniques. She has published over 16 papers in peer-reviewed international journals. Yang Liu was awarded the outstanding graduate student of Hunan University in 2016.

Liang Hu received his bachelor's degree of environmental engineering from Huazhong Agricultural University in 2013. He has received his master degree from Hunan University. Now, he is pursuing his PhD degree of analytical chemistry and biosensors aspects at Hunan University. His research interests include chemical/biological sensors and portable sensing platforms, especially with novel detection systems.

Yaoyu Zhou received his B.S. degree in Environmental Engineering from Jishou University, China in 2011. He received PhD degree in Hunan University, China under the guidance of Prof. Tang. He is currently teaching courses and performs research in College of Resources and Environment of Hunan Agricultural University, Changsha, China. His research interests include chemical/biological sensors and portable sensing platforms, especially with novel detection systems.